Full Paper
doi.org/10.1002/chem.202001357

Ligand Effects

A Phosphine Functionalized β-Diketimine Ligand for the Synthesis of Manifold Metal Complexes

Christina Zovko,[a] Sebastian Bestgen,[a, b] Christoph Schoo,[a] Anne Görner,[a] Jose M. Goicoechea,[b] and Peter W. Roesky*[a]

Abstract: A bis(diphenyl)-phosphine functionalized β-diketimine (PNac-H) was synthesized as a flexible ligand for transition metal complexes. The newly designed ligand features symmetrically placed phosphine moieties around a β-diketimine unit, forming a PNNP-type pocket. Due to the hard and soft donor atoms (N vs. P) the ligand can stabilize various coordination polyhedra. A complete series ranging from coordination numbers 2 to 6 was realized. Linear, trigonal planar, square planar, tetrahedral, square pyramidal, and octahedral coordination arrangements containing the PNac-ligand around the metal center were observed by using suitable metal sources. Hereby, PNac-H or its anion $PNac^-$ acts as mono-, bi- and tetradendate ligand. Such a broad flexibility is unusual for a rigid tetradentate system. The structural motifs were realized by treatment of PNac-H with a series of late transition metal precursors, for example, silver, gold, nickel, copper, platinum, and rhodium. The new complexes have been fully characterized by single crystal X-ray diffraction, NMR, IR, UV/Vis spectroscopy, mass spectrometry as well as elemental analysis. Additionally, selected complexes were investigated regarding their photophysical properties. Thus, PNac-H proved to be an ideal ligand platform for the selective coordination and stabilization of various metal ions in diverse polyhedra and oxidation states.

Introduction

Since the late 1960s, β-diketiminates (commonly known as NacNac) have been extensively studied and widely applied for the synthesis and stabilization of metal and non-metal compounds across the periodic table,[1–3] ranging from main group elements[4–7] to transition metals[8–10] as well as f-block elements.[11,12] β-Diketiminates are an omnipresent ligand system in coordination chemistry, mainly due to their convenient synthetic accessibility and easily adjustable scaffold, allowing a fine tuning of the electronic and steric environment.[13–16] This has led to a wide scope of applications[17] ranging from the formation of redox-active systems,[3] enhanced spectroscopic properties,[18] supporting ligands for metal-mediated catalysis[8,19–23] as well as the activation of small molecules.[13,24–26] In this regard, β-diketiminate ligands have been proven capable of supporting metal ions in a number of oxidation states as well as chemical environments.[27] Especially, the stabilization of sub-valent and uncommon oxidation states, for example, Fe^{I},[26] Al^{I},[24,27,28] Ga^{I},[27] Si^{II},[29] Ge^{I},[30] and Mg^{I} species,[31,32] has been an achievement of supporting β-diketiminate ligand systems. Hereby, the scaffold can be easily modified by varying the corresponding *N*-substituents, which are adjustable regarding their steric demand, electronic properties as well as the introduction of additional functionalities.[15] This offers a high degree of control for task-specific adjustments, for example, the kinetic stabilization of sub-valent and reactive metal species via sterically demanding substituents,[31,33,34] or an enhanced reactivity of the resulting metal complexes.[35,36]

In general, a β-diketiminate ligand provides a monoanionic, bidentate support for metal ions,[15] yet the introduction of additional heteroatom donor sites to the β-diketiminate scaffold allows the extension to more complex coordination motifs, a higher degree of metal stabilization as well as the potential formation of heterobimetallic complexes. Herein, the design of the ligand plays a crucial role in promoting or enforcing specific arrangements. The introduction of additional side groups to a β-diketimine system has already been investigated applying O-donor and S-donor functionalities (Figure 1), enabling the formation of multidentate ONNO and SNNS pockets, respectively. These bifunctional ligands were subsequently applied, for example, for the coordination of main group, transition and f-block elements.[37–39,41] Additionally, such bifunctional ligand systems may allow the combination of different transition

[a] C. Zovko, Dr. S. Bestgen, Dr. C. Schoo, A. Görner, Prof. P. W. Roesky
Institute of Inorganic Chemistry
Karlsruhe Institute of Technology (KIT)
Engesserstraße 15, 76131 Karlsruhe (Germany)
E-mail: roesky@kit.edu

[b] Dr. S. Bestgen, Prof. J. M. Goicoechea
Department of Chemistry, Chemistry Research Laboratory
University of Oxford
12 Mansfield Road, Oxford, OX1 3TA (UK)

Supporting information and the ORCID identification number(s) for the author(s) of this article can be found under: https://doi.org/10.1002/chem.202001357.

© 2020 The Authors. Published by Wiley-VCH GmbH. This is an open access article under the terms of Creative Commons Attribution NonCommercial License, which permits use, distribution and reproduction in any medium, provided the original work is properly cited and is not used for commercial purposes.

© 2020 The Authors. Published by Wiley-VCH GmbH

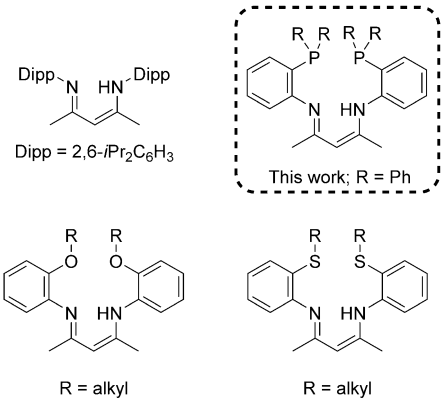

Figure 1. A series of β-diketimines (NacNac-H), applicable as ligands for the synthesis of metal complexes. The introduction of additional side groups, for example, O-donor[37,38] or S-donor[39,40] functionalities, allows the formation of specific coordinative pockets. In the case of additional phosphine side groups a PNNP pocket is formed.

metals within an organometallic structure, a research field which has been comprehensively studied in recent years.[42–44] To the best of our knowledge, related phosphine functionalized β-diketimine systems (see Figure 1, top right), exhibiting a PNNP type pocket, have not been reported yet. As phosphines are one of the most commonly applied ligand systems in coordination chemistry, a combination of these two moieties in one ligand would open new avenues for bifunctional ligand chemistry. Thus, phosphine functionalized β-diketimines seem advantageous for the synthesis of sophisticated metal complexes, as they shall be able to selectively coordinate via different bonding modes by their hard ketiminate and soft phosphine donor centers.[45,46]

Herein, we report the multigram scale synthesis of a novel bis(diphenyl)-phosphine functionalized β-diketimine (PNac-H, **1**) and its application as a bifunctional system. The additional phosphine donor sites of the NacNac type ligand form a PNNP pocket, thus allowing the selective coordination and stabilization of various metal centers by different coordination motifs. Due to the hard and soft donor atoms (N vs. P) PNac-H or its anion PNac$^-$ can stabilize various coordination polyhedra

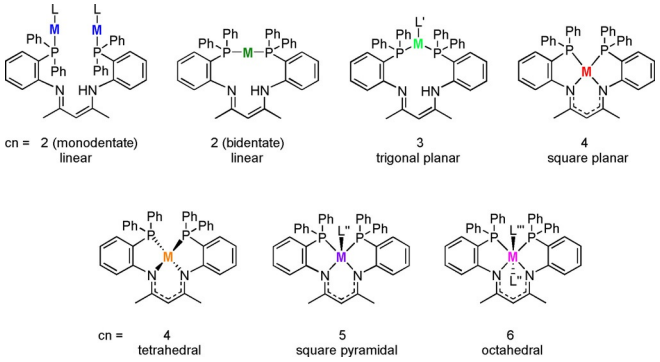

Figure 2. Coordination modes of the bifunctional PNac-H ligand (**1**) or its anion PNac$^-$ both reported herein for mono- and bimetallic complexes. Coordination numbers (cn) of the respective metal ions in the range from 2–6 were stabilized by this system (L, L′, L″, L‴ = other ligands). Seven different coordination polyhedral have been realized.

(Figure 2). A complete series of complexes ranging from coordination numbers (cn) 2 to 6 was realized. Such a broad flexibility in complex design is unusual for a rigid tetradentate ligand.

Results and Discussion

The phosphine functionalized β-diketimine ligand (**1**) was obtained by a two-step synthesis route in a multigram scale (Scheme 1). In the first step, a fluorine functionalized NacNac ligand (FNac-H) was formed by a condensation reaction between acetylacetone and 2-fluoroaniline in refluxing toluene.[47] Subsequently, FNac-H was reacted with freshly prepared $KPPh_2$, to obtain the novel bis-phosphine β-diketimine ligand **1** (PNac-H).

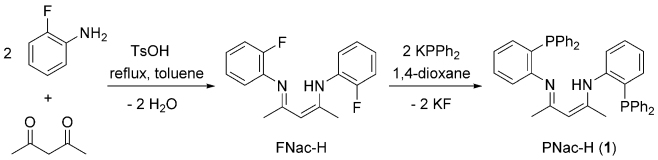

Scheme 1. Synthesis of PNac-H ligand (**1**) via a two-step reaction.

Single crystals of **1** were obtained by slow evaporation of a MeOH/DCM solution, allowing characterization by X-ray diffraction. Compound **1** crystallizes in the triclinic space group $P\bar{1}$ with one molecule in the asymmetric unit. The molecular structure of **1** in the solid state, as depicted in Figure 3, reveals the expected phosphine functionalized 1,3-diketimine structure. The angle of the diketimine backbone (C1-C2-C3) is 126.2(2)°, which is in the expected range for a protonated NacNac system.[14]

The composition of the bifunctional ligand **1** was further analyzed by NMR, IR and UV/Vis spectroscopy. In the $^{31}P\{^1H\}$ NMR spectrum ($CDCl_3$) of **1**, a single resonance is detected at $\delta = -14.5$ ppm, which displays the typical range for non-coordinated triarylphosphine moieties and indicates a symmetrical arrangement of both phosphine moieties in solution. In the ^1H NMR spectrum a characteristic resonance for the N-H moiety is detected at $\delta = 12.02$ ppm and for the methine moiety of the diketimine backbone at $\delta = 4.52$ ppm. The ^1H and $^{13}C\{^1H\}$ NMR spectra are consistent with proton migration

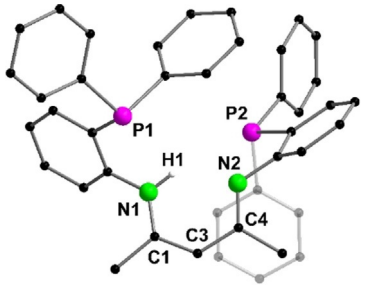

Figure 3. Molecular structure of **1** in the solid state. Carbon bound hydrogen atoms are omitted for clarity.

© 2020 The Authors. Published by Wiley-VCH GmbH

between the two nitrogen atoms of **1** in solution, a common phenomenon for related β-diketimine ligands. This results in a single set of resonances for each of the remaining phenyl and methyl groups.

The bifunctional PNac-H ligand, exhibiting a diketimine center and symmetrically attached phosphine units, enables the subsequent coordination of various metal ions. Moreover, the two different functionalities form a PNNP pocket, which allows a very flexible metal coordination resulting in seven different coordination polyhedra. The corresponding metal complexes are discussed herein with increasing coordination number.

Two-fold coordination

To realize a low coordinate linear coordination polyhedron, in which **1** acts a monodentate ligand, **1** was reacted with two equivalents of $[AuC_6F_5(tht)]$ (tht = tetrahydrothiophene) (Scheme 2). Hereby a neutral bimetallic Au^I complex [PNac-H-$(Au^IC_6F_5)_2$] (**2**) was obtained by ligand exchange reactions. Hereby, the weakly bound tht ligands are readily substituted by the two phosphine moieties of the PNac-H scaffold.[48]

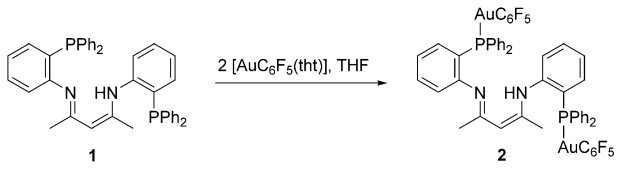

Scheme 2. Synthesis of the bimetallic Au^I complex **2**, from PNac-H (**1**) and two equivalents of $[AuC_6F_5(tht)]$.

Single crystals of **2** were obtained from slow diffusion of *n*-pentane into a DCM solution. Complex **2** crystallizes in the triclinic space group $P\bar{1}$, with one molecule in the asymmetric unit. Each phosphine moiety coordinates to a Au^I species, realizing a homobimetallic complex (Figure 4), in which **1** acts twice as monodentate donor. The molecular structure of **2** indicates that no intra- or intermolecular aurophilic interactions are present in the solid state. Instead, both Au^I fragments are spatially separated from each other and orientated in different directions. The Au^I centers are ligated in an almost linear fashion, as indicated by the P-Au-C_6F_5 bond angles (P1-Au1-C42 177.94(9)° and P2-Au2-C48 173.16(8)°). The gold phosphorous bond lengths in **2** (Au1–P1 2.2724(7), Au2–P2 2.2793(7) Å) are similar and in the same range as comparable Au^I phosphine complexes.[49–52]

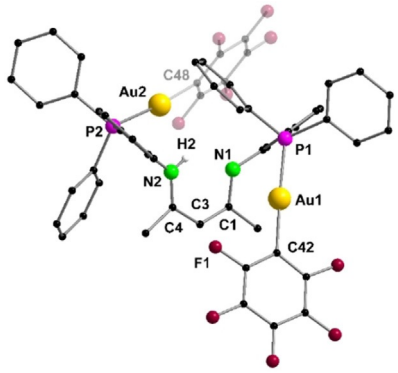

Figure 4. Molecular structure of **2** in the solid state. Carbon bound hydrogen atoms and solvent molecules (DCM) are omitted for clarity.

The composition of **2** was further confirmed by multinuclear NMR measurements (^1H, $^{13}C\{^1H\}$, $^{31}P\{^1H\}$, ^{19}F) as well as IR spectroscopy. In the ^1H NMR spectrum ([D_8]THF) a resonance for the N-H functionality is observed at $\delta = 11.58$ ppm. In the $^{31}P\{^1H\}$ NMR spectrum a single resonance is detected at $\delta =$ 33.8 ppm with the splitting of a pseudo-quintet. The resonance's chemical shift lies in the expected range for a triarylphosphine Au^I compound, confirming a sole phosphine-gold coordination.[48,50] The resonance splitting is caused by a long-range coupling to the fluorine atoms of the C_6F_5 moieties, an effect, which has already been observed in comparable $Au^IC_6F_5$ phosphine complexes.[50,53,54] Additionally, in the $^{19}F\{^1H\}$ NMR spectrum of **2**, a set of resonances for the C_6F_5 units, with an integration ratio of 2:1:2, is observed in the upfield region ($\delta =$ −117.7 to −166.0 ppm). The coordination of AuC_6F_5 to the phosphine units was also monitored by IR spectroscopy. The IR spectrum of **2** exhibits, in comparison to PNac-H, amongst others vibration bands at $\tilde{\nu} = 1048$ and 951 cm^{-1}, which can be attributed to the pentafluorophenyl moieties.[55] Additional bands, attributed to the skeletal vibrations of the perfluorated ring moieties, are observed in the region of $\tilde{\nu} =$ 1400–1500 cm^{-1}.

To realize a coordination mode, in which PNac-H acts as bidentate ligand, **1** was reacted with the group 11 metal precursors $Ag[BF_4]$ and $[Au(tht)_2][ClO_4]$, respectively (Scheme 3). Applying the Ag^I precursor, [PNac-H-Ag^I][BF_4] (**3**) is formed via a selective phosphine silver(I) coordination. In case of the Au^I species, [PNac-H-Au^I][ClO_4] (**4**) is formed accordingly by tht elimination.

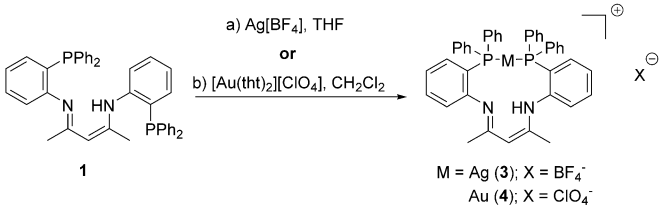

Scheme 3. Synthesis of the complexes **3** and **4** from the phosphine functionalized PNac-H (**1**) and group 11 metal precursors $Ag[BF_4]$ or $[Au(tht)_2][ClO_4]$.

Single crystals were obtained from slow diffusion of *n*-pentane (**3**) or diethyl ether (**4**) into a DCM solution of the corresponding substances, allowing analysis by X-ray diffraction. Both complexes crystallize in the monoclinic space group *Cc*, in each case with one molecule in the asymmetric unit. The corresponding molecular structures of **3** and **4** in the solid state are isostructural (Figure 5), containing their respective

© 2020 The Authors. Published by Wiley-VCH GmbH

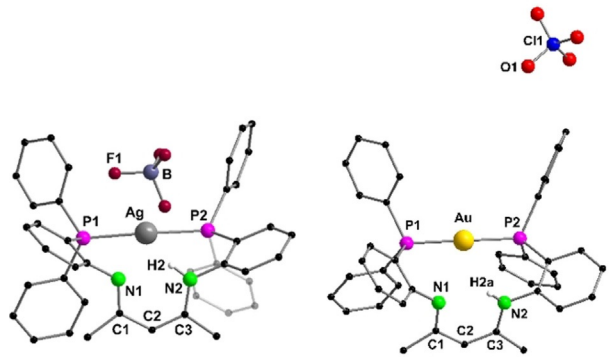

Figure 5. Molecular structures of **3** (left) and **4** (right) in the solid state. Carbon bound hydrogen atoms and solvent molecules (DCM) are omitted for clarity.

counterions ClO_4^- and BF_4^-. The Ag^I and Au^I center is ligated in an almost linear fashion as indicated by the P1-M-P2 bond angles (P1-Ag-P2 166.06(3)°, P1-Au-P2 175.08(5)°), yet the Ag^I structure deviates more from an ideal 180° alignment. This linear arrangement is expected for the d^{10}-electron systems Au^I and Ag^I. The soft metal ions are selectively coordinated by the soft phosphorus atoms (HSAB theory).[56] Thus, the β-diketimine pocket remains uncoordinated. The gold phosphorous distances in **4** (Au–P1 2.3069(13), Au–P2 2.3212(14) Å) are shorter in comparison to the silver phosphorous bond distances in **3** (Ag–P1 2.3818(9), Ag–P2 2.3994(9) Å), yet slightly longer than those in **2** (Au1–P1 2.2724(7), Au2–P2 2.2793(7) Å). The obtained data of both structures is in line with comparable bis-triarylphosphine complexes of Ag^I and Au^I.[57–59]

Furthermore, the isostructural compounds **3** and **4** were investigated by NMR and IR spectroscopy. In the $^{31}P\{^1H\}$ NMR spectrum ($CDCl_3$) of Au^I compound **4** a single resonance, significantly downfield shifted compared to ligand **1** ($\delta = -14.5$ ppm), is detected at $\delta = 34.5$ ppm, indicating a sole symmetric phosphine gold interaction.[60] In comparison, the $^{31}P\{^1H\}$ NMR spectrum ([D_8]THF) of Ag^I compound **3** exhibits two doublet resonances at $\delta = 1.2$ ppm, due to a coupling with the two Ag isotopes ^{107}Ag (d, $^2J_{P,Ag(107)} = 518.8$ Hz) and ^{109}Ag (d, $^2J_{P,Ag(109)} = 598.7$ Hz).[58,61] Additionally, a minor second set of resonances in the splitting of two doublets is observed at $\delta = -5.3$ ppm (d, $^2J_{P,Ag(107)} = 477.8$ Hz; d, $^2J_{P,Ag(109)} = 527.7$ Hz). This is may be due to a solvent effect of coordinating THF molecules in solution (Supporting Information, Figure S22). In the corresponding ^1H NMR spectra, a resonance for the N-H functionalities is observed accordingly at $\delta = 11.18$ ppm (**3**) and $\delta = 12.08$ ppm (**4**). As expected, the IR spectra of the isostructural compounds **3** and **4** are almost identical, with the exception of the vibrational modes of their respective counterions.[62]

Three-fold coordination

To realize a coordination number of 3, we aimed at the synthesis of a trigonal planar metal complex. Therefore, PNac-H was reacted with one equivalent of Pd^0 precursor [$Pd(PPh_3)_4$] (Scheme 4).

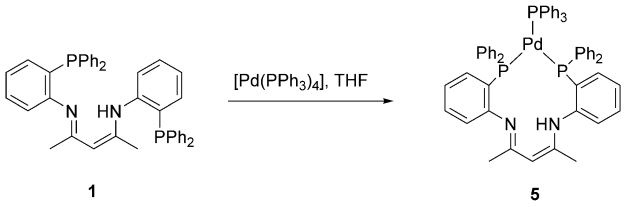

Scheme 4. Synthesis of palladium(0) complex **5** from PNac-H (**1**) and [$Pd(PPh_3)_4$].

Yellow single crystals of **5** suitable for X-ray analysis were obtained by slow diffusion of *n*-pentane into a toluene solution. Complex **5** crystallizes in the tetragonal space group $I4_1/a$, with one molecule in the asymmetric unit. The molecular structure of **5** in the solid state (Figure 6) confirms the substitution of three triphenylphosphine moieties of the Pd^0 precursor by the two outer phosphine units of the PNac-H ligand in a chelating fashion, yielding complex [PNac-H-Pd^0-PPh_3].

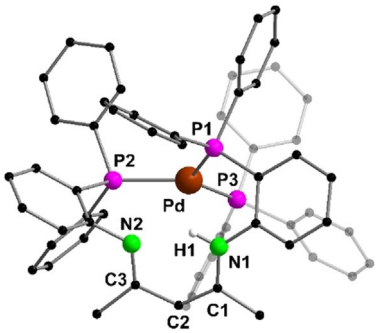

Figure 6. Molecular structure of **5** in the solid state. Carbon bound hydrogen atoms are omitted for clarity.

The Pd^0 center is ligated in a trigonal planar coordination sphere by both of the phosphine moieties of the PNac-H system and one triphenylphosphine ligand, indicated by the respective angles (P1-Pd-P2 117.07(4)°, P1-Pd-P3 121.64(4)°, P2-Pd-P3 120.26(4)°), which are close to an ideal arrangement of 120°. In **5**, all metal phosphorous bond lengths (Pd–P1 2.3075(11), Pd–P2 2.3010(10), Pd–P3 2.2981(11) Å) are almost identical, indicating a symmetric arrangement of the different ligand species in the solid state.[63,64]

Furthermore, compound **5** was analyzed by NMR and IR spectroscopy. In the $^{31}P\{^1H\}$ NMR spectrum ([D_8]THF) of **5** two resonances are detected at $\delta = 10.8$ ppm (d, $^2J_{P,P} = 83.0$ Hz) and $\delta = 25.9$ ppm (t, $^2J_{P,P} = 83.3$ Hz), which can be attributed to the different phosphine species, confirming a symmetric coordination behavior in solution.[64] In the ^1H NMR spectrum, the resonance for the N-H functionality is observed at $\delta = 12.55$ ppm.

Four-fold coordination

To realize a four-fold coordinated complex exhibiting a mono valent metal cation, PNac-H was reacted with one equivalent of the Ni^0 precursor [$Ni(cod)_2$] (cod = cyclooctadiene), obtaining

© 2020 The Authors. Published by Wiley-VCH GmbH

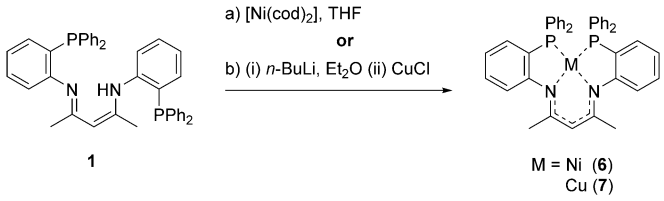

Scheme 5. Synthesis of the monometallic complexes **6** and **7** from PNac-H (**1**) and $[Ni(cod)_2]$ or CuCl (following prior deprotonation), respectively.

the complex [PNac-Ni^{I}] (**6**) by a redox reaction (Scheme 5). In a further approach, PNac-H was first deprotonated with *n*BuLi and subsequently reacted with copper(I) chloride to obtain [PNac-Cu^{I}] (**7**).

Dark-red single crystals of **6** suitable for X-ray analysis were obtained from slow diffusion of *n*-pentane into a THF solution, whereas compound **7** was crystallized by cooling a diethyl ether solution to 0 °C. Both complexes **6** and **7** crystallize in the monoclinic space group $P2_1/n$ with one molecule in the asymmetric unit. The molecular structures in the solid state (Figure 7) reveal a fourfold coordination of the Ni^{I} and Cu^{I} centers, respectively. Hereby, the corresponding metal ion is coordinated by both phosphine moieties as well as the nitrogen atoms of the diketiminate unit.

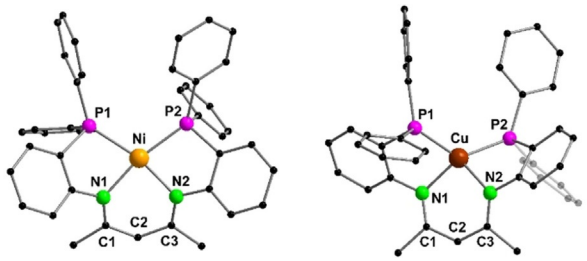

Figure 7. Molecular structures of **6** (left) and **7** (right) in the solid state. Hydrogen atoms are omitted for clarity.

In the Ni^{I} compound **6**, the Ni-P bond lengths are nearly identical and in the expected range (Ni–P1 2.2709(6), Ni–P2 2.2403(6) Å). A similar symmetric arrangement is seen for Ni–N bond lengths (Ni–N1 2.028(2), Ni–N2 2.042(2) Å).[65–67] The Ni^{I} center is formally in a square planar coordination sphere, as indicated by the respective angles (N1-Ni-N2 86.95(7°); P1-Ni-P2 111.13(2)°), deviating slightly from an ideal 90°, which is a result of the rigid nature of the ligand. Importantly, as it has been reported for different β-diketiminate systems, the PNNP pocket of the PNac ligand stabilizes the nickel center in its uncommon oxidation state of +1.[65,68]

In contrast to **6**, the copper(I) center in complex **7** is not coordinated in a square planar fashion, yet rather in a tetrahedral motif, with a phosphine bite angle of P1-Cu-P2 129.08(2)°. However, the respective angles (e.g., N1-Cu-P2 137.75(5)°, P1-Cu-N2 129.53(5)°) deviate significantly from an ideal tetrahedral arrangement of 109.5°, which may be due to the phosphines' rather limited degree of freedom. The corresponding Cu–P (Cu-P1 2.2222(5), Cu–P2 2.2483(5) Å) and Cu–N (Cu–N1 2.028(2), Cu–N2 2.027(2) Å) distances are in the same range as for **6** and in agreement to comparable tetradentate PNNP Cu^{I} complexes.[69–71] The angle of the β-diketiminate backbone (C1-C2-C3) is 127.6(2)° (**6**) and 131.5(2)° (**7**), hence being slightly elongated upon metal coordination (for **1**: 126.2(2)°).

The composition and structural arrangement of compounds **6** and **7** was further analyzed by NMR and IR spectroscopy as well as mass spectrometry. Due to the paramagnetic Ni^{I} moiety, merely broad resonances are detected in the corresponding NMR spectra of **6**, which are hardly interpretable. By applying the Evans NMR method,[72,73] the paramagnetic susceptibility of **6** in THF solution was determined, which is consistent with a complex containing a single unpaired electron, as for a d^9 Ni^{I} species (see Supporting Information). Applying EI (EI = electron ionization) mass spectrometry a signal at m/z = 675.095 $[M]^+$ (100%) can be detected corresponding to the positively charged complex **6**.

In the $^{31}P\{^1H\}$ NMR spectrum (C_6D_6) of diamagnetic Cu^{I} compound **7**, a single resonance at $\delta = -16.7$ ppm is observed. The upfield signal is in the same region as the uncoordinated PNac-H ligand ($\delta = -14.5$ ppm, $CDCl_3$), yet in agreement to Cu^{I} phosphine complexes of the type $[Cu(PPh_3)_3X]$ (X = Cl, Br, I)[74] and other bis-triarylphosphine Cu^{I} complexes.[71] Accordingly, in the ^1H NMR spectrum of **7**, no resonance for a N-H functionality is observed anymore, whereas a resonance for the methine moiety of the diketiminate backbone is detected at δ = 4.37 ppm (**1**: δ = 4.52 ppm).

In a subsequent approach for four-fold coordinated divalent metal cations, PNac-H was reacted with $[PtCl_2(dmso)_2]$ (dmso = dimethyl sulfoxide) and $Na[BF_4]$, after prior deprotonation with NaOMe. Hereby, the charged Pt^{II} complex [PNac-Pt^{II}][BF_4] (**8**) was formed (Scheme 6).

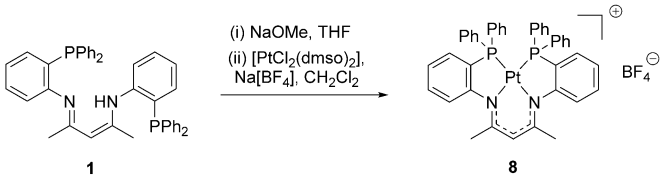

Scheme 6. Synthesis of platinum(II) complex **8** from PNac-H (**1**) and $[PtCl_2(dmso)_2]$ and $NaBF_4$, following prior deprotonation of PNac-H with NaOMe.

Red single crystals suitable for X-ray analysis were obtained by adding diethyl ether to a DCM solution of **8** and cooling it to −30 °C. Compound **8** crystallizes in the monoclinic space group $P2_1/n$ with one molecule in the asymmetric unit. The corresponding molecular structure in the solid state is depicted in Figure 8 and reveals a tetradentate square planar coordination geometry around the Pt^{II} center, as it is expected for a $4d^8$-electron system,[75] with the respective BF_4^- counterion.

However, in contrast to Ni^{I} compound **6**, the bite angles of the donors (P1-Pt-P2 100.88(3)°, N1-Pt-N2 93.25(10)°, N1-Pt-P1 82.39(7)°, N2-Pt-P2 84.52(8)°) are closer to an ideal 90°, forming

© 2020 The Authors. Published by Wiley-VCH GmbH

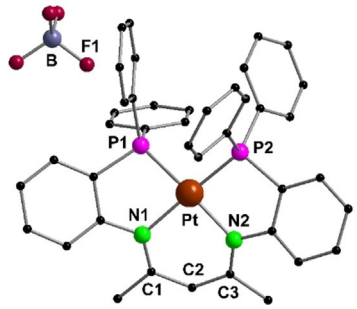

Figure 8. Molecular structure of **8** in the solid state. Hydrogen atoms and solvent molecules (DCM) are omitted for clarity.

a highly symmetric square planar coordination motif. In **8** the platinum phosphorous (Pt–P1 2.2338(8), Pt–P2 2.2334(8) Å) and platinum nitrogen bond lengths (Pt–N1 2.071(2), Pt–N2 2.053(2) Å) are in the same range as for the previously discussed complexes **6** and **7**. It is also in agreement with data for literature known Pt^{II} PNNP-type complexes.[76–78] The angle of the β-diketiminate backbone (C1-C2-C3 131.6(3)°) is similar to the one observed for Cu^{I} compound **7**.

The composition of **8** in solution was furthermore analyzed by multinuclear NMR spectroscopy (^{1}H, $^{13}C\{^{1}H\}$, $^{31}P\{^{1}H\}$ ^{195}Pt, ^{11}B, ^{19}F). $^{31}P\{^{1}H\}$ NMR measurements ($CDCl_3$) of **8** confirmed a symmetrical square planar platinum(II) coordination, as a single resonance at $\delta = 19.4$ ppm and the corresponding ^{195}Pt satellites (d, $^{1}J_{P,Pt} = 3178.5$ Hz), which are due to a coupling with the NMR active ^{195}Pt isotopes (33.8%, $s = {}^{1}/_{2}$), are observed.[77] This resonance pattern can be assigned to a square planar coordinated Pt^{II} moiety with two triarylphosphines in *cis*-configuration,[79] as it is depicted in the solid state structure. In comparison to PNac-H ($\delta = -14.5$ ppm), the main ^{31}P resonance is significantly downfield shifted upon coordination to the metal center.

Further, ^{195}Pt NMR spectroscopy was employed as a complementary analytical method. Here, a triplet resonance is detected at $\delta = -4068.0$ ppm (t, $^{1}J_{Pt,P} = 3183.9$ Hz) which can be assigned to the *cis*-configurated platinum(II) moiety.[80,81] This supports the results obtained by $^{31}P\{^{1}H\}$ NMR measurements (Supporting Information, Figure S37).

Five-fold coordination

To realize a five-fold coordinated complex, PNac-H was yet again reacted with one equivalent of the Ni^{0} precursor $[Ni(cod)_2]$. However, in this case the reaction was performed in dichloromethane instead of THF. During the reaction, the solution color changed from dark red to green, as it is expected for a Ni^{II} species. Most likely, Ni^{I} complex **6** is formed in situ, which then is rapidly oxidized by the chloride containing solvent, obtaining the divalent Ni complex [PNac-Ni^{II}-Cl] (**9**) (Scheme 7). This assumption was confirmed, as Ni^{II} complex **9** was also accessible starting from Ni^{I} species **6**.

Dark-green single crystals suitable for X-ray analysis were obtained by slow diffusion of diethyl ether to a DCM solution of **9**. Compound **9** crystallizes in the triclinic space group $P\bar{1}$ with

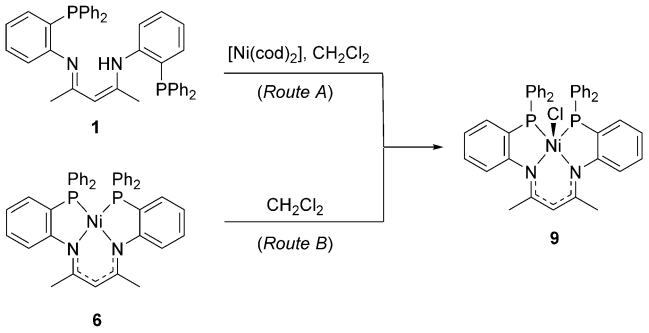

Scheme 7. Synthesis of Ni^{II} complex **9** from PNac-H (**1**) and $[Ni(cod)_2]$ in DCM (Route A). Alternatively, complex **9** can be synthesized, applying Ni^{I} compound **6** as starting material (Route B).

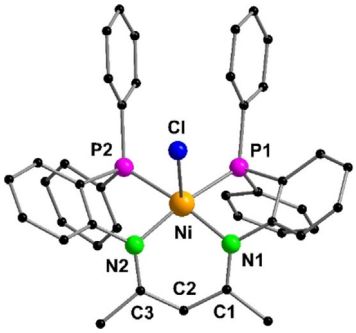

Figure 9. Molecular structure of **9** in the solid state. Hydrogen atoms are omitted for clarity.

one molecule in the asymmetric unit. The corresponding molecular structure in the solid state (Figure 9) reveals a square planar pyramidal coordination geometry around the Ni^{II} center,[82] consisting of the PNac ligand and a chloride. Hereby the tetradentate PNNP pocket coordinates in a square planar fashion (P1-Ni-P2 101.09(4)°, N1-Ni-N2 93.06(12)°) as it has already been observed in Ni^{I} complex **6**. Additionally, the chloride is positioned orthogonally to this plane, as indicated by the respective angles (e.g. P2-Ni-Cl 89.49(3)°, N2-Ni-Cl 93.90(8)°). The metal phosphorous (Ni–P1 2.1717(10), Ni–P2 2.1527(10) Å) and metal nitrogen bond lengths (Ni–N1 1.930(3), Ni–N2 1.933(3) Å) of **9** are both about 0.1 Å shorter than the Ni^{I} complex **6**, which is most likely due to the higher oxidation state of the nickel center and a difference in ionic radii between Ni^{I} and Ni^{II}.[66]

Compound **9** was also characterized by NMR and IR spectroscopy. In contrast to **6**, complex **9** allowed a meaningful characterization via NMR, confirming the presence of a diamagnetic Ni^{II} species. In the $^{31}P\{^{1}H\}$ NMR spectrum ($CDCl_3$) a single resonance at $\delta = 35.2$ ppm, significantly downfield shifted compared to ligand **1** ($\delta = -14.5$ ppm), is detected, indicating a symmetric phosphine nickel coordination in solution.

Six-fold coordination

To obtain a six-fold coordinated metal complex, PNac-H was reacted with a half of an equivalent of the dimeric metal precur-

© 2020 The Authors. Published by Wiley-VCH GmbH

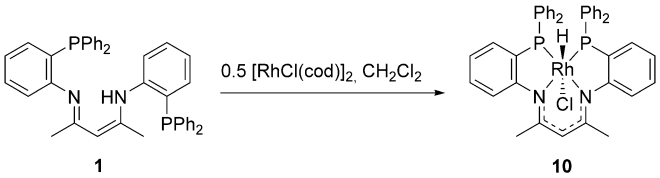

1 10

Scheme 8. Synthesis of rhodium(III) complex **10** from PNac-H (**1**) and the dimeric metal precursor $[RhCl(cod)]_2$.

sor $[RhCl(cod)]_2$. Upon insertion into the PNac-H backbone and substitution of cod by the phosphine groups, [PNac-Rh^{III}-Cl(H)] (**10**) is formed (Scheme 8).

Violet single crystals of **10**, suitable for X-ray analysis, were obtained from slow diffusion of diethyl ether into a DCM solution of the respective substance. Compound **10** crystallizes in the monoclinic space group $P2_1/n$, with one molecule in the asymmetric unit. The corresponding molecular structure of **10** in the solid state is depicted in Figure 10. Interestingly, an oxidative addition of the rhodium takes place along with a substitution of the cod ligand, resulting in the formation of a fix-fold coordinated Rh hydride species. The Rh^{III} center is formally in an octahedral coordination sphere, composed of two phosphines, two nitrogen atoms, a chloride and a hydride, thus forming the Rh^{III} complex [PNac-Rh^{III}-Cl(H)].

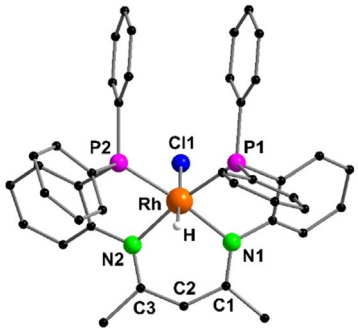

Figure 10. Molecular structure of **10** in the solid state. Hydrogen atoms (except Rh-H) and solvent molecules (DCM) are omitted for clarity.

In **10**, the respective metal phosphorous and metal nitrogen bonds are nearly identical and within the range of the previously discussed compounds. They also match with literature values of comparable Rh^{III} hydride complexes.[83–86] The bond angles P1-Rh-P2 104.74(3)° and N1-Rh-N2 91.06(10)° as well as Cl1-Rh-H 173(2)° indicate a relatively symmetric octahedral coordination sphere of the Rh^{III} center.

Complex **10** was further investigated by NMR and IR spectroscopy. Due to a coupling to the NMR active ^{103}Rh nucleus ($s = 1/2$), a doublet resonance at $\delta = 39.1$ ppm (d, $^1J_{P,Rh} = 119.1$ Hz) is detected in the $^{31}P\{^1H\}$ NMR spectrum (CD_2Cl_2) of **10**.[87,88] Additionally, in the ^{1}H NMR spectrum a resonance in the upfield region at $\delta = -13.92$ ppm (dt, $^1J_{H,Rh} = 21.4$ Hz, $^2J_{H,P} = 18.1$ Hz) is seen, which can be attributed to the Rh hydride species (see Figure S44).[84,86,88] Further, the IR spectrum of compound **10** exhibits absorption bands in the region of $\tilde{\nu} =$ 2040–2080 cm^{-1} which are characteristic for a Rh-H vibration and in-line with literature data.[85,89,90]

Photophysical properties

Metal complexes **5**–**10** exhibit characteristic colors, ranging from yellow to red and green. On the other hand, Au^I and Ag^I compounds **2**–**4** are obtained as colorless crystals, showing no absorption in the visible range. Hence, UV/Vis absorption spectra of PNac-H (**1**) and **5**–**10** were recorded in THF or DCM solution at room temperature (see Supporting Information; Figures S58–S64). Correspondingly, they demonstrate distinctive absorption bands in the visible spectral range. The bifunctional ligand PNac-H shows a pronounced absorption band between $\lambda = 320$–380 nm ($\lambda_{max.} = 354$ nm). Moreover, there are dominant absorption transitions in the UV region (< 300 nm) for all investigated complexes. For Pd^0 and Ni^I complexes **5** and **6**, a local absorption maximum is observed around $\lambda = 373$ (**5**) and 411 nm (**6**), hence being slightly red-shifted upon metal coordination compared to PNac-H. Measurements of the Cu^I complex **7** exhibited two local absorption bands at $\lambda = 393$ and 515 nm, whereas Pt^{II} compound **8** reveals only a weak absorption at $\lambda = 349$ nm and a dominant band at $\lambda = 498$ nm. UV/Vis analysis of Ni^{II} species **9** resulted in a local absorption band at $\lambda = 499$ nm, being significantly red-shifted in comparison to the Ni^I complex **6** ($\lambda = 411$ nm). Rh^{III} complex **10** displays two dominant absorptions bands at $\lambda = 379$ and 543 nm. The red-shifting as well as the appearance of new absorption bands, in comparison to PNac-H, can be qualitatively understood in terms of additional metal coordination, allowing amongst others MLCT (MLCT = metal to ligand charge transfer) processes.

Additionally, most complexes exhibited photoluminescence upon UV excitation. Thus, photoluminescent emission (PL) and excitation (PLE) spectra were recorded for compounds **1**–**5**, **8** and **10** in the solid state (see Supporting Information; Figures S65–S74), whereas **6**, **7** and **9** showed no significant PL. The PL and PLE spectra of PNac-H as well as metal complexes **8** and **10** are presented in Figure 11, recorded at 77 and 295 K. All emission bands are rather broad, with a full width at half maximum of about 100–200 nm. The main emission band of **1** is centered at 408 nm (at 77 K), which is significantly red-shifted and broadened at 295 K ($\lambda_{max.} = 474$ nm). Additionally, the PL intensity decreases at higher temperatures (spectra in Figure 11 are normalized). The PL of **1** can be attributed to fluorescence with a lifetime of about 2 ns (at both 77 K and 295 K). On the other hand, no long-lived emission (phosphorescence) was detected. For Pt^{II} complex **8**, an emission band at 630 nm (77 K) is observed upon radiation with 463 nm, which is barely shifted on increasing temperature (634 nm at 295 K). The emission mainly results from phosphorescence of **8** with $\tau = 64$ µs at 77 K and $\tau = 8$ µs at 295 K.

A weak fluorescence of **8** with a lifetime of 2 ns is observed at 417 nm, which is comparable with the fluorescence of the PNac-H ligand (detected at 416 nm). Rh^{III} complex **10** exhibits an emission band at 713 nm (77 K), which is, in contrast to PNac-H, blue-shifted at elevated temperature (672 nm at

© 2020 The Authors. Published by Wiley-VCH GmbH

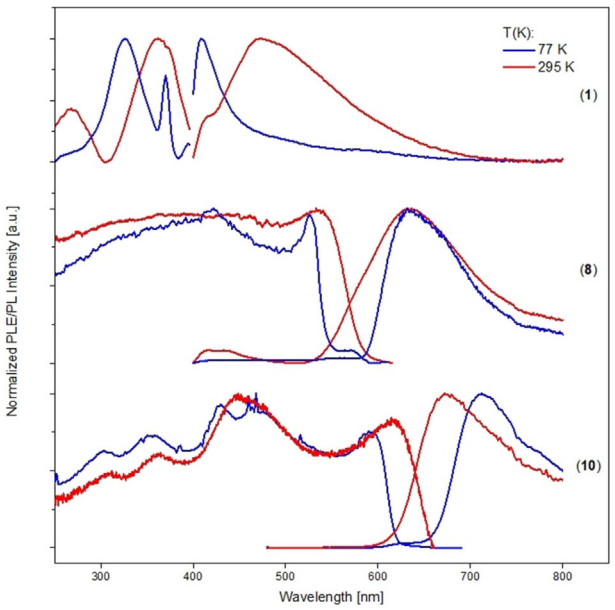

Figure 11. Photoluminescence excitation (PLE) and emission (PL) spectra of PNac-H (**1**), Pt^{II} complex **8** and Rh^{III} complex **10**, recorded at 77 K (blue) and 295 K (red). Spectra of complexes **2**–**5** are shown in the Supporting Information, Figures S67–S70).

298 K). Interestingly, complex **10** displays the highest emission red-shift of all investigated complexes and represents the only compound exhibiting no fluorescence. The long-lived emission of **10** has a lifetime of $\tau = 138$ µs at 77 K and $\tau = 8$ µs at 295 K. For the compounds **2**–**5** fluorescence is observed with a lifetime range of approximately 2–3 ns at 295 K, with respect to the particular excitation wavelength of each compound. Additionally, a weak phosphorescence ($\tau = 8$–10 µs) was detected at 295 K. In summary, PL spectra of **8** and **10** are both significantly red-shifted compared to PNac-H, which most likely originates from metal to ligand charge transfer excited states (bearing no excited ligand states). Similar qualitative observations were made for the metal complexes **3**–**5** (see Supporting Information). Again, a red shift in emission, compared to PNac-H, is observed for these compounds. In summary, each complex (**2**–**5**, **8** and **10**) exhibits a distinct emission spectrum, depending on the incorporated metal or complex fragment of the functionalized ligand system. The distinct luminescence of ligand **1** is quenched upon complexation of metal ions, yielding complexes, which show predominantly phosphorescent behavior. This effect is strongest for the incorporation of Rh^{III}, whereas Pt^{II} shows also traces of luminescence. Hence, new photoluminescent properties can be obtained by the implementation of a metal species to PNac-H. The emission lifetimes of the measured compounds **2**–**5**, **8** and **10** are in the range of nano to microseconds and in a typical range for ligand-assisted transition metals complexes. The observed phosphorescence is most likely facilitated by the spin orbit interactions of the heavy metal ions, allowing an intersystem crossing.[91]

Conclusions

In summary, we present the synthesis of a novel bis(diphenyl)-phosphine functionalized β-diketimine (**1**) and its application as a multipurpose ligand system. The symmetrically placed phosphine donor sites of the β-diketimine form an PNNP pocket, which subsequently allowed for the selective formation and stabilization of a series of late transition metal complexes (**2**–**10**) with coordination numbers ranging from 2 to 6. Herein, PNac-H or its anion $PNac^-$ act as mono, bi and tetradentate ligand. Depending on the applied metal precursor, diverse structural arrangements, such as linear, trigonal planar, square planar, tetrahedral, square pyramidal, and octahedral coordination arrangement of PNac-H or its anion $PNac^-$ were achieved. Hence, due to hard and soft donor atoms PNac-H proved to be an ideal ligand system for the coordination and stabilization of various metal ions in diverse oxidation states and coordination geometries.

Experimental Section

General procedures: All manipulations were performed under exclusion of moisture and oxygen in flame-dried Schlenk-type glassware or in an argon-filled *MBraun* glovebox. Prior to use, DCM was distilled under nitrogen from CaH_2. Hydrocarbon solvents (THF, Et_2O, *n*-pentane) were dried using an *MBraun* solvent purification system (SPS-800). THF was additionally distilled under nitrogen from potassium and benzophenone before storage over 4 Å molecular sieves. Analogously, 1,4-dioxane was distilled from potassium (after storage over KOH) and stored over 4 Å molecular sieves. Deuterated solvents were obtained from Carl Roth GmbH (99.5 atom % D). Prior to use, $CDCl_3$ and CD_2Cl_2 were stored over molecular sieves (4 Å), whereas [D_8]THF and C_6D_6 were stored over a NaK alloy. NMR spectra were recorded on a Bruker Avance II 300 MHz or Avance 400 MHz. ^1H and $^{13}C\{^1H\}$ NMR chemical shifts were referenced to the residual ^1H and ^{13}C resonances of the deuterated solvents and are reported relative to tetramethylsilane (TMS). $^{31}P\{^1H\}$ resonances are reported relative to external 85% phosphoric acid, ^{19}F resonances to $CFCl_3$, ^{11}B resonances to 15% $BF_3{\cdot}Et_2O$ in $CDCl_3$ and ^{195}Pt resonances relative to 1.2 M Na_2PtCl_6 in D_2O. IR spectra were obtained on a *Bruker* Tensor 37 FTIR spectrometer equipped with a room temperature DLaTGS detector and a diamond ATR (attenuated total reflection) unit. Elemental analyses were carried out with a Micro Cube from *Elementar Analysensysteme GmbH*. EI mass spectra were obtained from a *Thermofischer* DFS mass spectrometer. Ultraviolet-visible (UV/Vis) spectra were recorded on a *VARIAN* Cary 50 Scan UV/Visible spectrophotometer. Spectra were recorded in THF or DCM at room temperature and collected between 300 and 800 nm. Samples were baseline corrected with respect to the pure solvent. Photoluminescence measurements were performed with a PTI QuantaMaster™ 8000 series spectrometer, equipped with multiple illuminators and double emission monochromator with R928 PTM, InGaAs and InSb detector and a continuous 75 W xenon lamp. At 295 K the solid samples (crystalline powders) were measured as dispersions in a thin layer of viscous mineral oil (Sigma Aldrich), placed between 1 mm quartz plates (Material: Spectrosil®2000). Measurements at 77 K were recorded using a quartz cold finger dewar, passing light down to about 200 nm. The samples are measured in an EPR tube, which is placed in the liquid nitrogen filled dewar.

© 2020 The Authors. Published by Wiley-VCH GmbH

$[Au(tht)_2][ClO_4]$,[92] $[AuC_6F_5(tht)]$,[55] $[PtCl_2(dmso)_2]$[93] and FNac-H[47] were prepared according to literature procedures. $[AgBF_4]$ (99%), NaOMe (95%) and *n*BuLi (2.5 M in hexane) were purchased from Sigma–Aldrich. Bis(1,5-cyclooctadiene)dirhodium(I) dichloride and CuCl (99.99%) were purchased from Alfa Aesar. Diphenylphosphine (99%), $[Pd(PPh_3)_4]$ (99.9%), $[Ni(cod)]_2$ (98%) and $[NaBF_4]$ (98%) were purchased from abcr. Elemental potassium (98% in mineral oil) was purchased from Acros Organics. They were all used as received.

Synthesis[94,95]

General information: In the $^{13}C\{^1H\}$ NMR spectra of complexes **2**–**3**, **5** and **7**–**10** virtual triplet resonances (vt) are observed, due to specific C-P couplings. This fine structure splitting has previously been reported for organo-phosphorous metal complexes.[96–97] For complexes **2** and **8**, a ^{31}P decoupling has been applied, to simplify the evaluation of the ^{13}C NMR spectra. The corresponding NMR data are labelled as $^{13}C\{^1H, ^{31}P\}$.

PNac-H (1): Diphenylphosphine (4.28 mL, 4.58 g, 24.6 mmol, 3.00 equiv.) was dissolved in 1,4-dioxane (25 mL) at room temperature. Potassium chunks (963 mg, 24.6 mmol, 3.00 equiv.) were added and the mixture was stirred at 60 °C until the formation of $KPPh_2$ was complete (indicated by the visible absence of molten potassium; approx. 2 h). FNac-H (2.35 g, 8.20 mmol, 1.00 equiv.) was added as a solid and the resulting mixture was stirred at 100 °C for two days. Subsequently, the solvent was removed under reduced pressure. To the residue, water (25 mL) and dichloromethane (approx. 50 mL) were added as well as a few spatulas of Na_2CO_3, and the mixture stirred for 5 minutes. Then, the organic phase was separated, dried over Na_2SO_4 and filtered to obtain a clear solution. The solution was slightly concentrated to a volume of approximately 30 mL and then MeOH (30 mL) was added. Upon concentration of the solution under reduced pressure, **1** precipitated as a yellowish crystalline substance, which was separated by filtration und finally dried under vacuum. Yield: 2.40 g (48%).

^1H NMR ($CDCl_3$, 400 MHz): δ [ppm] = 1.55 (s, 6H, CH_3), 4.52 (s, 1H, CH_{NacNac}), 6.58 (ddd, $^3J_{H,H}$ = 7.9 Hz, $^3J_{H,H}$ = 4.5 Hz, $^4J_{H,H}$ = 1.3 Hz, 2H, CH_{Ar}) 6.67 (ddd, $^3J_{H,H}$ = 7.7 Hz, $^3J_{H,H}$ = 3.9 Hz, $^4J_{H,H}$ = 1.5 Hz, 2H, CH_{Ar}), 6.89 (td, $^3J_{H,H}$ = 7.5 Hz, $^4J_{H,H}$ = 1.2 Hz, 2H, CH_{Ar}), 7.06–7.16 (m, 22H, CH_{Ar}), 12.02 (s, 1H, NH). $^{13}C\{^1H\}$ NMR ($CDCl_3$, 101 MHz): δ [ppm] = 20.9 (CH_3), 96.9 (CH_{NacNac}), 124.1 (CH_{Ar}), 124.5 (CH_{Ar}), 128.2 (vt, $^2J_{C,P}$ = 6.9 Hz, CH_{Ar}), 128.3 (CH_{Ar}), 128.9 (CH_{Ar}), 132.7 (CH_{Ar}), 134.1 (d, $^2J_{C,P}$ = 20.8 Hz, CH_{Ar}), 137.3 (d, $^1J_{C,P}$ = 11.8 Hz, C_q), 137.3 (d, $^1J_{C,P}$ = 14.9 Hz, C_q), 149.1 (d, $^2J_{C,P}$ = 22.0 Hz, CN_q), 159.4 (CN_q). $^{31}P\{^1H\}$ NMR ($CDCl_3$, 162 MHz): δ [ppm] = −14.5 (s, PPh_2Ar). IR (ATR): $\tilde{\nu}$ [cm^{-1}] = 3049 (w), 3000 (vw), 2918 (vw), 1619 (s), 1537 (vs), 1484 (w), 1456 (w), 1429 (s), 1360 (vw), 1334 (vw), 1273 (m), 1182 (w), 1153 (vw), 1122 (vw), 1093 (vw), 1064 (vw), 1026 (w), 996 (vw), 918 (vw), 805 (vw), 765 (w), 738 (s), 692 (s), 633 (vw), 593 (vw), 496 (w), 464 (vw). Elemental analysis calcd (%) for $[C_{41}H_{36}N_2P_2]$ (618.76 g mol^{-1}): C 79.59, H 5.87, N 4.53; found C 79.45, H 5.68, N 4.71. UV/Vis: $\lambda_{max.(local)}$ [nm] = 354.

[PNac-H-($Au^IC_6F_5$)$_2$] (2): PNac-H (**1**) (150 mg, 0.24 mmol, 1.00 equiv.) and $[AuC_6F_5(tht)]$ (218 mg, 0.48 mmol, 2.00 equiv.) were dissolved in 10 mL THF and stirred for 16 hours at room temperature. Subsequently, the solvent was removed under reduced pressure and washed with *n*-pentane. Single crystals of **2** suitable for X-ray analysis were obtained from slow diffusion of *n*-pentane into a DCM solution. Crystalline yield: 217 mg (66%).

^1H NMR ([D$_8$]THF, 400 MHz): δ [ppm] = 1.42 (s, 6H, CH_3), 4.50 (s, 1H, CH_{NacNac}), 6.71 (ddd, $^3J_{H,H}$ = 11.1, $^3J_{H,H}$ = 7.8, $^4J_{H,H}$ = 1.4 Hz, 2H, CH_{Ar}), 6.82–6.88 (m, 2H, CH_{Ar}), 6.99–7.06 (m, 2H, CH_{Ar}), 7.23–7.58 (m, 22H, CH_{Ar}), 11.57 (s, 1H, NH). $^{13}C\{^1H\}$ NMR ([D$_8$]THF, 101 MHz): δ [ppm] = 21.6 (CH_3), 100.4 (CH_{NacNac}), 123.6 (C_q), 124.2 (C_q), 125.2 (d, $J_{C,P}$ = 8.5 Hz, CH_{Ar}), 127.8 (d, $J_{C,P}$ = 5.6 Hz, CH_{Ar}), 130.1 (d, $J_{C,P}$ = 10.9 Hz, CH_{Ar}), 131.9 (CH_{Ar}), 132.5 (CH_{Ar}), 134.2 (d, $J_{C,P}$ = 5.5 Hz, CH_{Ar}), 135.5 ($d_{(broad)}$, CH_{Ar}), 150.0 (d, $^2J_{C,P}$ = 10.0 Hz, CN_q), 162.2 (CN_q). Carbon atoms of the C_6F_5 moieties cannot be observed. $^{31}P\{^1H\}$ NMR ([D$_8$]THF, 162 MHz): δ [ppm] = 33.8 (pseudo-quintet, *P*-AuC_6F_5). ^{19}F NMR ([D$_8$]THF, 377 MHz): δ [ppm] = −117.7 to −114.2 (m, C_6F_5), −161.7 (t, $^3J_{F,F}$ = 19.8 Hz, C_6F_5), −166.0 to −163.2 (m, C_6F_5). IR (ATR): $\tilde{\nu}$ [cm^{-1}] = 3074 (vw), 3052 (vw), 1620 (m), 1586 (vw), 1564 (vw), 1531 (m), 1502 (s), 1484 (m), 1453 (vs), 1434 (vs), 1382 (vw), 1366 (w), 1351 (m), 1329 (vw), 1281 (w), 1268 (m), 1254 (m), 1183 (m), 1159 (w), 1123 (vw), 1102 (m), 1073 (m), 1059 (m), 1048 (m), 1028 (w), 999 (w), 951 (s), 922 (w), 872 (vw), 805 (vw), 791 (m), 766 (w), 741 (m), 711 (w), 690 (m), 593 (vw), 554 (w), 538 (vw), 508 (m), 481 (w). Elemental analysis calcd (%) for $[C_{53}H_{36}Au_2F_{10}N_2P_2{\cdot}CH_2Cl_2]$ (1431.68 g mol^{-1}): C 45.30, H 2.68, N 1.96; found C 45.04, H 2.68, N 2.07.

[PNac-H-Ag^I][BF_4] (3): PNac-H (**1**) (100 mg, 0.16 mmol, 1.00 equiv.) and $Ag[BF_4]$ (31.0 mg, 0.16 mmol, 1.00 equiv.) were dissolved in 10 mL THF 10 mL and stirred for 4 hours at room temperature, whereupon an off-white solid precipitated. The solvent was removed under reduced pressure and subsequently dissolved in 3 mL DCM. Single crystals suitable for X-ray analysis were obtained by slow diffusion of *n*-pentane into a solution of **3** in DCM. For NMR analysis the obtained crystals were dissolved and recrystallized in THF. Crystalline yield: 56.0 mg (43%).

^1H NMR ([D$_8$]THF, 400 MHz): δ [ppm] = 1.17 (s, 6H, CH_3), 4.52 (s, 1H, CH_{NacNac}), 7.00–7.09 (m, 4H, CH_{Ar}), 7.21 (t, $^3J_{H,H}$ = 7.6 Hz, 2H, CH_{Ar}), 7.4 –7.53 (m, 15H, CH_{Ar}), 7.55–7.67 (m, 7H, CH_{Ar}), 11.18 (s, 1H, NH). $^{13}C\{^1H, ^{31}P\}$ NMR ([D$_8$]THF, 101 MHz): δ [ppm] = 21.1 (CH_3), 98.0 (CH_{Nacnac}), 126.9 (CH_{Ar}), 127.3 (CH_{Ar}), 129.2 (C_q), 130.5 (CH_{Ar}), 132.3 (CH_{Ar}), 132.9 (CH_{Ar}), 133.9 (CH_{Ar}), 135.3 (C_q), 135.8 (CH_{Ar}), 149.5 (CN_q), 164.1 (CN_q). ^{11}B NMR ([D$_8$]THF, 128 MHz): δ [ppm] = −0.93 to −1.04 (m, BF_4). ^{19}F NMR ([D$_8$]THF, 377 MHz): δ [ppm] = −153.2 to −153.3 (m, BF_4). $^{31}P\{^1H\}$ NMR ([D$_8$]THF, 162 MHz): δ [ppm] = 1.2 (d, $^2J_{P,Ag(107)}$ = 518.8 Hz), 1.2 (d, $^2J_{P,Ag(109)}$ = 598.7 Hz).- An additional resonance in the $^{31}P\{^1H\}$ NMR spectrum can be detected at δ = −5.3 (d, $^2J_{P,Ag(107)}$ = 477.8 Hz), −5.3 (d, $^2J_{P,Ag(109)}$ = 527.7 Hz) which is attributed to a solvent coordinated species. IR (ATR): $\tilde{\nu}$ [cm^{-1}] = 3067 (vw), 3049 (vw), 3022 (vw), 2916 (vw), 1612 (m), 1580 (vw), 1525 (vs), 1479 (m), 1457 (w), 1432 (vs), 1375 (vw), 1333 (w), 1270 (s), 1185 (w), 1161 (vw), 1129 (vw), 1098 (s), 1072 (s), 1023 (vs), 993 (s), 920 (vw), 874 (vw), 802 (vw), 744 (s), 694 (vs), 599 (vw), 547 (vw), 517 (m), 485 (s), 438 (vw), 416 (vw). Elemental analysis calcd (%) for $[C_{41}H_{38}AgBF_4N_2P_2{\cdot}CH_2Cl_2]$ (898.30 g mol^{-1}): C 56.16, H 4.26, N 3.12; found C 56.56, H 4.66, N 3.06.

[PNac-H-Au^I][ClO_4] (4): PNac-H (**1**) (100 mg, 0.16 mmol, 1.00 equiv.) and $[Au(tht)_2][ClO_4]$ (76.0 mg, 0.16 mmol, 1.00 equiv.) were dissolved in 5 mL DCM and stirred for 1 hour at room temperature. Subsequently, the solution was concentrated to approximately 3 mL. Single crystals of **4** suitable for X-ray analysis were obtained from slow diffusion of diethyl ether into the DCM solution. Crystalline yield: 114.0 mg (78%).

^1H NMR ($CDCl_3$, 400 MHz): δ [ppm] = 1.31 (s, 6H, CH_3), 4.62 (s, 1H, CH_{NacNac}), 6.94–7.01 (m, 2H, CH_{Ar}), 7.09–7.16 (m, 2H, CH_{Ar}), 7.28–7.35 (m, 2H, CH_{Ar}), 7.52–7.66 (m, 22H, CH_{Ar}), 12.08 (s, 1H, NH). $^{13}C\{^1H\}$ NMR ($CDCl_3$, 101 MHz): δ [ppm] = 20.3 (CH_3), 97.1 (CH_{NacNac}), 125.4 (vt, $^1J_{C,P}$ = 31.7 Hz, C_q), 126.3 (vt, $J_{C,P}$ = 4.6 Hz, CH_{Ar}), 126.6 (vt, $J_{C,P}$ = 2.6 Hz, CH_{Ar}), 127.1 (vt, $^1J_{C,P}$ = 30.0 Hz, C_q), 130.5 (vt, $J_{C,P}$ = 5.9 Hz, CH_{Ar}), 132.9 (CH_{Ar}), 133.7 (CH_{Ar}), 133.9 (vt, $J_{C,P}$ = 3.4 Hz, CH_{Ar}), 134.3 (CH_{Ar}), 147.6 (vt, $^2J_{C,P}$ = 5.4 Hz, CN_q), 162.9 (CN_q). $^{31}P\{^1H\}$ NMR ($CDCl_3$, 162 MHz): δ [ppm] = 34.5 (s). IR (ATR): $\tilde{\nu}$ [cm^{-1}] = 3048 (w), 2988 (vw), 1614 (s), 1586 (vw), 1563 (vw), 1535 (vs), 1487 (w), 1460 (w),

© 2020 The Authors. Published by Wiley-VCH GmbH

1432 (vs), 1387 (vw),1354 (w), 1334 (vw), 1308 (vw), 1280 (w), 1255 (m), 1185 (w), 1159 (vw), 1129 (vw), 1093 (m), 1068 (vw), 1027 (vw), 996 (vw), 973 (vw), 919 (vw), 870 (vw), 800 (vw), 746 (s), 690 (vs), 590 (w), 555 (w), 511 (s), 486 (m), 436 (vw), 415 (vw). Elemental analysis calcd (%) for $[C_{41}H_{36}AuClN_2O_4P_2{\cdot}CH_2Cl_2]$ (1000.04 g mol^{-1}): C 50.44, H 3.83, N 2.80; found C 49.77, H 3.49, N 2.77.

[PNac-H-Pd^0-PPh$_3$] (5): PNac-H (**1**) (100 mg, 0.16 mmol, 1.00 equiv.) and $[Pd(PPh_3)_4]$ (184 mg, 0.16 mmol, 1.00 equiv.) were dissolved in 15 mL THF and stirred at room temperature for 16 h. Subsequently, the solvent was removed under reduced pressure to obtain an orange solid. Single crystals of **5** suitable for X-ray analysis were obtained by slow diffusion of *n*-pentane into a toluene solution. Crystalline yield: 82 mg (52%).

^{1}H NMR ([D$_8$]THF, 300 MHz): δ [ppm] = 1.36 (s, 6H, CH_3), 4.50 (s, 1H, CH_{NacNac}), 6.46–6.68 (m, 2H, CH_{Ar}), 6.78–7.00 (m, 17H, CH_{Ar}), 7.01–7.26 (m, 24H, CH_{Ar}), 12.55 (s, 1H, N*H*). ^{13}C{^{1}H} NMR ([D$_8$]THF, 75 MHz): δ [ppm] = 21.5 (*C*H$_3$), 97.8 (*C*H$_{NacNac}$), 101.6 (*C*H$_{Ar}$), 123.2 (*C*H$_{Ar}$), 123.4 (*C*H$_{Ar}$), 128.4 (vt, $J_{C,P}$ = 4.3 Hz, *C*H$_{Ar}$), overlapping signals 128.5–128.7 (*C*H$_{Ar}$) 128.8 (*C*H$_{Ar}$), 129.3 (*C*H$_{Ar}$), 132.8 (*C*H$_{Ar}$), 135.0 (d, $J_{C,P}$ = 17.6 Hz, *C*H$_{Ar}$), 135.3 (vt, $J_{C,P}$ = 9.2 Hz, *C*H$_{Ar}$), 139.4 (vt, $^1J_{C,P}$ = 10.1 Hz, C_q) 139.6 (C_q), 139.8 (C_q), 149.2 (vt, $^2J_{C,P}$ = 8.5 Hz, *C*N$_q$), 158.6 (*C*N$_q$). ^{31}P{^{1}H} NMR ([D$_8$]THF, 121 MHz): δ [ppm] = 10.8 (d, $^2J_{P,P}$ = 83.0 Hz, Pd-(*P*Ph$_2$Ar)$_2$), 25.9 (t, $^2J_{P,P}$ = 83.3 Hz, Pd-*P*Ph$_3$). IR (ATR): $\tilde{\nu}$ [cm^{-1}] = 3069 (vw), 3052 (w), 2997 (vw), 1628 (m), 1584 (vw), 1564 (w), 1150 (m), 1499 (vw), 1475 (w), 1454 (w), 1431 (s), 1383 (vw), 1359 (vw), 1305 (vw), 1276 (w), 1250 (w), 1233 (vw), 1185 (w), 1121 (vw), 1084 (w), 1065 (vw), 1026 (vw), 998 (vw), 984 (vw), 926 (vw), 864 (vw), 842 (vw), 799 (vw), 742 (s), 720 (w), 694 (vs), 675 (w), 618 (vw), 594 (vw), 541 (vw), 504 (vs), 495 (s), 476 (w), 417 (w). Elemental analysis calcd (%) for $[C_{59}H_{51}N_2P_3Pd]$ (987.41 g mol^{-1}): C 71.77, H 5.21, N 2.84; found C 70.83, H 5.16, N 2.75. UV/Vis: $\lambda_{max.(local)}$ [nm] = 373.

[PNac-Ni^I] (6): PNac-H (**1**) (100 mg, 0.16 mmol, 1.00 equiv.) and $[Ni(cod)_2]$ (45.0 mg, 0.16 mmol, 1.00 equiv.) were dissolved in 10 mL THF and stirred at room temperature for 6 hours. Then, the dark red solution was concentrated under reduced pressure to approximately 3 mL. Single crystals of **6** suitable for X-ray analysis were obtained from slow diffusion of *n*-pentane into a THF solution. Crystalline yield: 63.0 mg (58%).

IR (ATR): $\tilde{\nu}$ [cm^{-1}] = 3050 (w), 2976 (vw), 2916 (vw), 2856 (vw), 1629 (vw), 1579 (w), 1552 (vw), 1526 (w), 1504 (vw), 1478 (vw), 1432 (s), 1376 (vs), 1356 (vs), 1308 (w), 1266 (s), 1233 (m), 1181 (m), 1153 (m), 1121 (s), 1095 (m), 1065 (w), 1022 (w), 998 (w), 980 (w), 932 (vw), 858 (vw), 816 (vw), 744 (s), 717 (m), 692 (s), 619 (vw), 547 (m), 524 (w), 498 (w), 469 (vw), 429 (vw). Elemental analysis calcd (%) for $[C_{41}H_{35}N_2NiP_2{\cdot}C_4H_8O]$ (748.49 g mol^{-1}): C 72.21, H 5.79, N 3.74; found C 71.19, H 5.88, N 3.75. EI-MS (70 eV, QT = 150 °C): *m/z* [%] = 675.095 [M]$^+$ (100). UV/Vis: $\lambda_{max.(local)}$ [nm] = 411. Due to paramagnetic Ni^I moiety, merely broad resonances can be detected in the corresponding ^{1}H, ^{13}C{^{1}H} and ^{31}P{^{1}H} NMR spectra, which are not interpretable.

[PNac-Cu^I] (7): PNac-H (**1**) (100 mg, 0.16 mmol, 1.00 equiv.) was dissolved in 10 mL diethyl ether and the corresponding solution cooled to −78 °C. After this 0.07 mL *n*BuLi (2.5 M, 0.16 mmol, 1.00 equiv.) was added to the solution and stirred for 30 minutes. Then, Cu^{I}Cl (16.0 mg, 0.16 mmol, 1.00 equiv.) was added at room temperature. After stirring for another 16 h, whereupon a white solid precipitated, the solution was concentrated to approximately 5 mL and subsequently filtered through a PTFE filter. Single crystals of **7** suitable for X-ray analysis were obtained by cooling the diethyl ether solution to 0 °C. Crystalline yield: 45.0 mg (41%).

^{1}H{^{31}P} NMR (C_6D_6, 300 MHz): δ [ppm] = 1.73 (s, 6H, CH_3), 4.37 (s, 1H, CH_{NacNac}), 6.70 (td, $^3J_{H,H}$ = 7.3 Hz, $^4J_{H,H}$ = 1.3 Hz, 2H, CH_{Ar}), 6.92–7.04 (m, 14H, CH_{Ar}), 7.06–7.15 (m, 4H, CH_{Ar}), 7.51–7.56 (m, 8H, CH_{Ar}). ^{13}C{^{1}H} NMR (C_6D_6, 75 MHz): δ [ppm] = 22.4 (*C*H$_3$), 97.2 (*C*H$_{NacNac}$), 100.7 (*C*H$_{Ar}$), 121.7 (*C*H$_{Ar}$), 121.9 (*C*H$_{Ar}$), 128.6 (vt, $J_{C,P}$ = 4.4 Hz, *C*H$_{Ar}$), 129.1 (*C*H$_{Ar}$), 129.7 (*C*H$_{Ar}$), 132.3 (*C*H$_{Ar}$), 134.1 (vt, $J_{C,P}$ = 8.6 Hz, *C*H$_{Ar}$), 134.7 (d, $^1J_{C,P}$ = 42.3 Hz, C_q), 134.9 (vt, $^1J_{C,P}$ = 12.3 Hz, C_q), 156.4 (vt, $^2J_{C,P}$ = 8.8 Hz, *C*N$_q$), 161.3 (*C*N$_q$). ^{31}P{^{1}H} NMR (C_6D_6, 121 MHz): δ [ppm] = −16.7 (s). IR (ATR): $\tilde{\nu}$ [cm^{-1}] = 3071 (vw), 3049 (vw), 2996 (vw), 2912 (vw), 1581 (vw), 1543 (m), 1520 (vw), 1482 (vw), 1437 (m), 1386 (vs), 1376 (vs), 1350 (s), 1298 (w), 1257 (w), 1182 (m), 1155 (vw), 1121 (vw), 1093 (vw), 1062 (vw), 1023 (w), 937 (vw), 864 (vw), 815 (vw), 767 (vw), 740 (m), 692 (m), 606 (w), 555 (vw), 529 (vw), 502 (w), 476 (w), 425 (vw). Elemental analysis calculated (%) for $[C_{41}H_{35}CuN_2P_2]$ (681.24 g mol^{-1}): C 72.29, H 5.18, N 4.11; found C 72.32, H 4.85, N 4.11. UV/Vis: $\lambda_{max.(local)}$ [nm] = 393, 515.

[PNac-Pt^{II}][BF$_4$] (8): PNac-H (**1**) (100 mg, 0.16 mmol, 1.00 equiv.) and NaOMe (9.00 mg, 0.16 mmol, 1.00 equiv.) were dissolved in 10 mL THF and stirred overnight. Subsequently, the solvent was removed under reduced pressure and the resulting solid washed with diethyl ether. Then, $[PtCl_2(dmso)_2]$ (68.0 mg, 0.16 mmol, 1.00 equiv.) and Na[BF$_4$] (18.0 mg, 0.16 mmol, 1.00 equiv.) were added to the solid. The mixture was dissolved in 5 mL DCM and the solution stirred for 2 hours at room temperature. Single crystals of **8** suitable for X-ray analysis were obtained by adding 10 mL diethyl ether to the DCM solution and subsequent cooling to −30 °C. Crystalline yield: 88.0 mg (61%).

^{1}H NMR ($CDCl_3$, 400 MHz): δ [ppm] = 2.25 (s, 6H, CH_3), 5.10 (s, 1H, CH_{NacNac}), 6.93–6.99 (m, 2H, CH_{Ar}), 7.02–7.07 (m, 2H, CH_{Ar}), 7.13 (dd, $^3J_{H,H}$ = 8.3 Hz, $^3J_{H,H}$ = 3.6 Hz, 2H, CH_{Ar}), 7.18–7.26 (m, 16H, CH_{Ar}), 7.39–7.47 (m, 6H, CH_{Ar}). ^{13}C{^{1}H, ^{31}P} NMR ($CDCl_3$, 101 MHz): δ [ppm] = 24.2 (*C*H$_3$), 113.9 (*C*H$_{NacNac}$), 123.8 (*C*H$_{Ar}$), 124.1 (C_q), 125.2 (C_q), 125.8 (*C*H$_{Ar}$), 129.5 (*C*H$_{Ar}$), 132.6 (*C*H$_{Ar}$), 132.8 (*C*H$_{Ar}$), 133.0 (*C*H$_{Ar}$), 133.2 (*C*H$_{Ar}$), 158.2 (*C*N$_q$), 160.2 (*C*N$_q$). ^{31}P{^{1}H} NMR ($CDCl_3$, 162 MHz): δ [ppm] = 19.4 (d, $^1J_{P,Pt}$ = 3178.5 Hz). ^{11}B NMR ($CDCl_3$, 128 MHz): δ [ppm] = −0.79 to −0.84 (m, *B*F$_4$). ^{19}F NMR ($CDCl_3$, 377 MHz): δ [ppm] = −154.5 to −154.7 (m, B*F*$_4$). ^{195}Pt NMR ($CDCl_3$, 86 MHz): δ [ppm] = −4068.0 (t, $^1J_{Pt,P}$ = 3183.9 Hz). IR (ATR): $\tilde{\nu}$ [cm^{-1}] = 3056 (vw), 1580 (vw), 1566 (vw), 1533 (w), 1518 (w), 1482 (vw), 1454 (w), 1431 (m), 1377 (w), 1351 (vs), 1310 (vw), 1268 (s), 1251 (w), 1198 (vw), 1184 (vw), 1165 (vw), 1139 (vw), 1105 (w), 1066 (m), 1046 (m), 1033 (s), 1022 (s), 997 (w), 947 (vw), 877 (vw), 852 (vw), 785 (vw), 760 (w), 742 (w), 729 (w), 715 (w), 701 (w), 691 (m), 634 (vw), 567 (w), 552 (w), 531 (w), 516 (w), 502 (w), 428 (vw). Elemental analysis calcd (%) for $[C_{41}H_{37}PtBF_4N_2P_2{\cdot}CH_2Cl_2]$ (984.51 g mol^{-1}): C 51.24, H 3.79, N 2.85; found C 51.23, H 4.11, N 2.77. UV/Vis: $\lambda_{max.(local)}$ [nm] = 349, 498.

[PNac-Ni^{II}-Cl] (9): (*Route A*): PNac-H (**1**) (150 mg, 0.24 mmol, 1.00 equiv.) and $[Ni(cod)_2]$ (66.0 mg, 0.24 mmol, 1.00 equiv.) were dissolved in 10 mL DCM and stirred over night at 30 °C. Then, the dark green solution was concentrated under reduced pressure to approximately 3 mL. Single crystals of **9** suitable for X-ray analysis were obtained from slow diffusion of diethyl ether into the DCM solution. Crystalline yield: 113 mg (65%).- (*Route B*): Alternatively, complex **9** can be synthesized, reacting Ni^I compound **6** with DCM, applying similar reaction conditions.

^{1}H NMR ($CDCl_3$, 400 MHz): δ [ppm] = 2.05 (s, 6H, CH_3), 5.31 (s, 1H, CH_{NacNac}), 6.81–6.98 (m, 6H, CH_{Ar}), 7.21–7.31 (m, 8H, CH_{Ar}), 7.33–7.42 (m, 10H, CH_{Ar}), 7.48 (t, $^3J_{H,H}$ = 7.6 Hz, 4H, CH_{Ar}). ^{13}C{^{1}H} NMR ($CDCl_3$, 101 MHz): δ [ppm] = 22.6 (*C*H$_3$), 115.5 (*C*H$_{NacNac}$), 123.7 (vt, $J_{C,P}$ = 6.0 Hz, *C*H$_{Ar}$), 124.7 (vt, $^1J_{C,P}$ = 25.6 Hz, C_q), 125.1 (vt, $J_{C,P}$ = 3.8 Hz, *C*H$_{Ar}$), 129.5 (vt, $J_{C,P}$ = 5.4 Hz, *C*H$_{Ar}$), 126.6 (vt, $^1J_{C,P}$ = 27.9 Hz, C_q),

© 2020 The Authors. Published by Wiley-VCH GmbH

131.4 (CH_{Ar}), 132.2 (CH_{Ar}), 133.1 (vt, $J_{C,P}=5.2$ Hz, CH_{Ar}), 133.2 (CH_{Ar}), 156.9 (vt, $^2J_{C,P}=11.6$ Hz, CN_q), 160.4 (CN_q). $^{31}P\{^1H\}$ NMR ($CDCl_3$, 162 MHz): δ [ppm] = 35.2 (s). IR (ATR): $\tilde{\nu}$ [cm^{-1}] = 3050 (w), 2985 (vw), 1578 (vw), 1574 (vw), 1543 (m), 1523 (m), 1481 (vw), 1454 (m), 1435 (s), 1372 (s), 1356 (vs), 1345 (vs), 1303 (vw), 1268 (s), 1192 (w), 1158 (vw), 1132 (vw), 1097 (m), 1069 (vw), 1032 (w), 1019 (m), 997 (vw), 946 (vw), 928 (w), 759 (m), 740 (m), 720 (m), 690 (s), 635 (vw), 567 (vw), 541 (w), 524 (vw), 509 (m), 497 (m), 480 (vw). Elemental analysis calcd (%) for [$C_{41}H_{35}N_2NiP_2Cl{\cdot}0.25\,CH_2Cl_2$] (733.07 g mol^{-1}): C 67.59, H 4.88, N 3.82; found C 67.50, H 5.40, N 3.69. UV/Vis: $\lambda_{max.(local)}$ [nm] = 499.

[PNac-Rh^{III}-Cl(H)] (10): PNac-H (**1**) (100 mg, 0.16 mmol, 1.00 equiv.) and $[RhCl(cod)]_2$ (40.0 mg, 0.08 mmol, 0.50 equiv.) were dissolved in 10 mL DCM and stirred for 3 hours at room temperature. Then, the violet solution was concentrated under reduced pressure to approximately 3 mL. Single crystals of **10** suitable for X-ray analysis were obtained from slow diffusion of diethyl ether into the DCM solution. Crystalline yield: 46.0 mg (37%).

^1H NMR (CD_2Cl_2, 400 MHz): δ [ppm] = −13.92 (dt, $^1J_{H,Rh}=21.4$ Hz, $^2J_{H,P}=18.1$ Hz, 1H, Rh-*H*), 2.10 (s, 6H, CH_3), 4.77 (s, 1H, CH_{NacNac}), 6.78–6.87 (m, 6H, CH_{Ar}), 6.97–7.06 (m, 4H, CH_{Ar}), 7.15 (t, $^3J_{H,H}=7.4$ Hz, 2H, CH_{Ar}) 7.23–7.29 (m, 6H, CH_{Ar}), 7.36 (t, $^3J_{H,H}=7.3$ Hz, 4H, CH_{Ar}), 7.46 (t, $^3J_{H,H}=7.3$ Hz, 2H, CH_{Ar}), 7.56–7.61 (m, 4H, CH_{Ar}). $^{13}C\{^1H\}$ NMR (CD_2Cl_2, 101 MHz): δ [ppm] = 23.9 (CH_3), 111.7 (CH_{NacNac}), 122.9 (C_q), 124.4 (vt, $J_{C,P}=6.6$ Hz, C_q), 128.1 (vt, $J_{C,P}=5.2$ Hz, CH_{Ar}), 129.0 (vt, $J_{C,P}=5.1$ Hz, CH_{Ar}), 130.7 (d, $J_{C,P}=59.1$ Hz, CH_{Ar}), 131.2 (CH_{Ar}), 132.6 (CH_{Ar}), 133.6 (vt, $J_{C,P}=5.8$ Hz, CH_{Ar}), 134.3 (vt, $J_{C,P}=5.1$ Hz, CH_{Ar}), 158.6 (vt, $^2J_{C,P}=9.3$ Hz, CN_q), 161.6 (CN_q). $^{31}P\{^1H\}$ NMR (CD_2Cl_2, 162 MHz): δ [ppm] = 39.1 (d, $^1J_{P,Rh}=119.1$ Hz). IR (ATR): $\tilde{\nu}$ [cm^{-1}] = 3051 (vw), 2958 (vw), 2922 (vw), 2080 (vw), 2040 (vw), 1577 (vw), 1543 (w), 1518 (vw), 1482 (vw), 1430 (m), 1376 (w), 1349 (s), 1308 (m), 1262 (s), 1233 (vs), 1190 (vs), 1152 (vs), 1125 (s), 1094 (m), 1064 (vw), 1023 (w), 980 (m), 945 (vw), 864 (vw), 839 (vw), 806 (vw), 758 (w), 743 (w), 694 (m), 637 (vw), 619 (vw), 548 (w), 503 (m). Elemental analysis calcd (%) for [$C_{41}H_{36}RhN_2P_2{\cdot}2\,CH_2Cl_2$] (926.91 g mol^{-1}): C 55.72, H 4.35, N 3.02; found C 55.33, H 4.24, N 3.08. UV/Vis: $\lambda_{max.(local)}$ [nm] = 379, 543.

X-ray crystallographic studies: Detailed XRD measurement description as well as crystal and structure refinement data are provided as Supporting Information. Additionally, selected bond lengths and angles of all compounds (**1**–**10**) are given in the Supporting Information (Figures S1–S10).

Associated Content: Supporting Information: Additional XRD and structure refinement data; selected bond lengths and angles of all compounds; NMR- and IR- spectra of every compound; mass and UV/Vis spectra of selected compounds.

Deposition numbers 1989054, 1989055, 1989056, 1989057, 1989058, 1989059, 1989060, 19890601, 1989062, and 1989063 contain(s) the supplementary crystallographic data for this paper. These data are provided free of charge by the joint Cambridge Crystallographic Data Centre and Fachinformationszentrum Karlsruhe Access Structures service.

Acknowledgements

Financial support by the DFG-funded transregional collaborative research center SFB/TRR 88 "Cooperative Effects in Homo and Heterometallic Complexes (3MET)", project C3, is gratefully acknowledged. S.B. gratefully acknowledges the Deutsche Forschungsgemeinschaft (DFG, BE 6401/1-1) (Project 380155090) for a generous fellowship. T. J. Feuerstein and M. Dahlen are acknowledged for their help regarding the photophysical measurements and N. D. Knöfel for helpful discussions and NMR evaluation. Open access funding enabled and organized by Projekt DEAL.

Conflict of interest

The authors declare no conflict of interest.

Keywords: coordination polyhedra · phosphine · photophysical properties · PNNP · β-diketimine

[1] S. G. McGeachin, *Can. J. Chem.* **1968**, *46*, 1903.
[2] J. E. Parks, R. H. Holm, *Inorg. Chem.* **1968**, *7*, 1408.
[3] C. Camp, J. Arnold, *Dalton Trans.* **2016**, *45*, 14462.
[4] M. H. Chisholm, J. C. Huffman, K. Phomphrai, *J. Chem. Soc. Dalton Trans.* **2001**, 222.
[5] Y. Yang, P. M. Gurubasavaraj, H. Ye, Z. Zhang, H. W. Roesky, P. G. Jones, *J. Organomet. Chem.* **2008**, *693*, 1455.
[6] M. E. Desat, R. Kretschmer, *Z. Anorg. Allg. Chem.* **2020**, https://doi.org/10.1002/zaac.201900193.
[7] M. E. Desat, R. Kretschmer, *Dalton Trans.* **2019**, *48*, 17718.
[8] F. Lauterwasser, P. G. Hayes, S. Bräse, W. E. Piers, L. L. Schafer, *Organometallics* **2004**, *23*, 2234.
[9] J. Vela, J. M. Smith, Y. Yu, N. A. Ketterer, C. J. Flaschenriem, R. J. Lachicotte, P. L. Holland, *J. Am. Chem. Soc.* **2005**, *127*, 7857.
[10] P. H. M. Budzelaar, R. de Gelder, A. W. Gal, *Organometallics* **1998**, *17*, 4121.
[11] D. V. Vitanova, F. Hampel, K. C. Hultzsch, *J. Organomet. Chem.* **2005**, *690*, 5182.
[12] Y. Yao, Y. Zhang, Z. Zhang, Q. Shen, K. Yu, *Organometallics* **2003**, *22*, 2876.
[13] Y.-C. Tsai, *Coord. Chem. Rev.* **2012**, *256*, 722.
[14] M. Stender, R. J. Wright, B. E. Eichler, J. Prust, M. M. Olmstead, H. W. Roesky, P. P. Power, *J. Chem. Soc. Dalton Trans.* **2001**, 3465.
[15] L. Bourget-Merle, M. F. Lappert, J. R. Severn, *Chem. Rev.* **2002**, *102*, 3031.
[16] C. Chen, S. M. Bellows, P. L. Holland, *Dalton Trans.* **2015**, *44*, 16654.
[17] R. M. Gauld, R. McLellan, A. R. Kennedy, J. Barker, J. Reid, R. E. Mulvey, *Chem. Eur. J.* **2019**, *25*, 14728.
[18] Y. K. Radwan, A. Maity, T. S. Teets, *Inorg. Chem.* **2015**, *54*, 7122.
[19] M. Cheng, A. B. Attygalle, E. B. Lobkovsky, G. W. Coates, *J. Am. Chem. Soc.* **1999**, *121*, 11583.
[20] R. L. Webster, *Dalton Trans.* **2017**, *46*, 4483.
[21] B. M. Chamberlain, M. Cheng, D. R. Moore, T. M. Ovitt, E. B. Lobkovsky, G. W. Coates, *J. Am. Chem. Soc.* **2001**, *123*, 3229.
[22] C. Weetman, M. S. Hill, M. F. Mahon, *Chem. Eur. J.* **2016**, *22*, 7158.
[23] A. S. S. Wilson, M. S. Hill, M. F. Mahon, *Organometallics* **2019**, *38*, 351.
[24] Y. Liu, J. Li, X. Ma, Z. Yang, H. W. Roesky, *Coord. Chem. Rev.* **2018**, *374*, 387.
[25] K. C. MacLeod, D. J. Vinyard, P. L. Holland, *J. Am. Chem. Soc.* **2014**, *136*, 10226.
[26] F. Spitzer, C. Graβl, G. Balázs, E. M. Zolnhofer, K. Meyer, M. Scheer, *Angew. Chem. Int. Ed.* **2016**, *55*, 4340; *Angew. Chem.* **2016**, *128*, 4412.
[27] M. Zhong, S. Sinhababu, H. W. Roesky, *Dalton Trans.* **2020**, *49*, 1351.
[28] C. Cui, H. W. Roesky, H.-G. Schmidt, M. Noltemeyer, H. Hao, F. Cimpoesu, *Angew. Chem. Int. Ed.* **2000**, *39*, 4274; *Angew. Chem.* **2000**, *112*, 4444.
[29] M. Driess, S. Yao, M. Brym, C. van Wüllen, D. Lentz, *J. Am. Chem. Soc.* **2006**, *128*, 9628.
[30] W. D. Woodul, E. Carter, R. Müller, A. F. Richards, A. Stasch, M. Kaupp, D. M. Murphy, M. Driess, C. Jones, *J. Am. Chem. Soc.* **2011**, *133*, 10074.
[31] C. Jones, *Nat. Rev. Chem.* **2017**, *1*, 0059.
[32] C. Jones, L. McDyre, D. M. Murphy, A. Stasch, *Chem. Commun.* **2010**, *46*, 1511.
[33] N. M. Rajendran, A. Haleel, N. D. Reddy, *Organometallics* **2014**, *33*, 217.
[34] M. Arrowsmith, B. Maitland, G. Kociok-Köhn, A. Stasch, C. Jones, M. S. Hill, *Inorg. Chem.* **2014**, *53*, 10543.
[35] S. F. McWilliams, P. L. Holland, *Acc. Chem. Res.* **2015**, *48*, 2059.

© 2020 The Authors. Published by Wiley-VCH GmbH

[36] R. E. Cowley, P. L. Holland, *Inorg. Chem.* **2012**, *51*, 8352.
[37] R. Olejník, Z. Padělková, A. Fridrichová, M. Horáček, J. Merna, A. Růžička, *J. Organomet. Chem.* **2014**, *759*, 1.
[38] S. M. Barbon, V. N. Staroverov, P. D. Boyle, J. B. Gilroy, *Dalton Trans.* **2014**, *43*, 240.
[39] S. Pfirrmann, C. Limberg, E. Hoppe, *Z. Anorg. Allg. Chem.* **2009**, *635*, 312.
[40] O. Sanganas, S. Löscher, S. Pfirrmann, N. Marinos, P. Glatzel, T.-C. Weng, C. Limberg, M. Driess, H. Dau, M. Haumann, *J. Phys. Conf. Ser.* **2009**, *190*, 012199.
[41] T. D. Thangadurai, K. Natarajan, *Transit. Met. Chem.* **2002**, *27*, 485.
[42] D. W. Stephan, *Coord. Chem. Rev.* **1989**, *95*, 41.
[43] P. Buchwalter, J. Rosé, P. Braunstein, *Chem. Rev.* **2015**, *115*, 28.
[44] J. A. Mata, F. E. Hahn, E. Peris, *Chem. Sci.* **2014**, *5*, 1723.
[45] R. G. Pearson, *J. Chem. Educ.* **1968**, *45*, 581.
[46] R. G. Pearson, *J. Chem. Educ.* **1968**, *45*, 643.
[47] T. Li, W. Song, H. Ai, Q. You, A. Zhang, G. Xie, *J. Polym. Res.* **2015**, *22*, 631.
[48] S. Bestgen, M. T. Gamer, S. Lebedkin, M. M. Kappes, P. W. Roesky, *Chem. Eur. J.* **2015**, *21*, 601.
[49] T. Tanase, R. Otaki, T. Nishida, H. Takenaka, Y. Takemura, B. Kure, T. Nakajima, Y. Kitagawa, T. Tsubomura, *Chem. Eur. J.* **2014**, *20*, 1577.
[50] S. Bestgen, C. Schoo, C. Zovko, R. Köppe, R. P. Kelly, S. Lebedkin, M. M. Kappes, P. W. Roesky, *Chem. Eur. J.* **2016**, *22*, 7115.
[51] R. W. Baker, P. J. Pauling, *J. Chem. Soc. Dalton Trans.* **1972**, 2264.
[52] T. Simler, P. Braunstein, A. A. Danopoulos, *Dalton Trans.* **2016**, *45*, 5122.
[53] X. C. Cambeiro, T. C. Boorman, P. Lu, I. Larrosa, *Angew. Chem. Int. Ed.* **2013**, *52*, 1781; *Angew. Chem.* **2013**, *125*, 1825.
[54] N. D. Knöfel, C. Schweigert, T. J. Feuerstein, C. Schoo, N. Reinfandt, A.-N. Unterreiner, P. W. Roesky, *Inorg. Chem.* **2018**, *57*, 9364.
[55] R. Uson, A. Laguna, M. Laguna, D. A. Briggs, H. H. Murray, J. P. Fackler, *(Tetrahydrothiophene)Gold(I) or Gold(III) Complexes*, Wiley, Hoboken, **2007**.
[56] R. G. Pearson, *J. Am. Chem. Soc.* **1963**, *85*, 3533.
[57] E. Wächtler, S. H. Privér, J. Wagler, T. Heine, L. Zhechkov, M. A. Bennett, S. K. Bhargava, *Inorg. Chem.* **2015**, *54*, 6947.
[58] R. E. Bachman, D. F. Andretta, *Inorg. Chem.* **1998**, *37*, 5657.
[59] A. Bayler, A. Schier, G. A. Bowmaker, H. Schmidbaur, *J. Am. Chem. Soc.* **1996**, *118*, 7006.
[60] M. C. Gimeno, A. Laguna, *Chem. Rev.* **1997**, *97*, 511.
[61] A. Del Zotto, P. Di Bernardo, M. Tolazzi, G. Tomat, P. Zanonato, *J. Chem. Soc. Dalton Trans.* **1993**, 3009.
[62] M. R. Tchalala, J. K. El-Demellawi, E. Abou-Hamad, J. R. D. Retamal, P. Varadhan, J.-H. He, S. Chaieb, *Appl. Mater. Today* **2017**, *9*, 10.
[63] A. L. Casalnuovo, J. C. Calabrese, *J. Am. Chem. Soc.* **1990**, *112*, 4324.
[64] W. Lesueur, E. Solari, C. Floriani, A. Chiesi-Villa, C. Rizzoli, *Inorg. Chem.* **1997**, *36*, 3354.
[65] P. L. Holland, T. R. Cundari, L. L. Perez, N. A. Eckert, R. J. Lachicotte, *J. Am. Chem. Soc.* **2002**, *124*, 14416.
[66] A. Hashimoto, H. Yamaguchi, T. Suzuki, K. Kashiwabara, M. Kojima, H. D. Takagi, *Eur. J. Inorg. Chem.* **2010**, 39.
[67] C. L. Rock, T. L. Groy, R. J. Trovitch, *Dalton Trans.* **2018**, *47*, 8807.
[68] C.-Y. Lin, P. P. Power, *Chem. Soc. Rev.* **2017**, *46*, 5347.
[69] X. Li, J. Ding, W. Jin, Y. Cheng, *Inorg. Chim. Acta* **2009**, *362*, 233.
[70] N. Carrera, N. Savjani, J. Simpson, D. L. Hughes, M. Bochmann, *Dalton Trans.* **2011**, *40*, 1016.
[71] M. Schulz, F. Dröge, F. Herrmann-Westendorf, J. Schindler, H. Görls, M. Presselt, *Dalton Trans.* **2016**, *45*, 4835.
[72] D. F. Evans, *J. Chem. Soc.* **1959**, 2003.
[73] K. De Buysser, G. G. Herman, E. Bruneel, S. Hoste, I. Van Driessche, *Chem. Phys.* **2005**, *315*, 286.
[74] J. V. Hanna, S. E. Boyd, P. C. Healy, G. A. Bowmaker, B. W. Skelton, A. H. White, *Dalton Trans.* **2005**, 2547.
[75] S. O. Grim, R. L. Keiter, W. McFarlane, *Inorg. Chem.* **1967**, *6*, 1133.
[76] S. Burger, B. Therrien, G. Süss-Fink, *Eur. J. Inorg. Chem.* **2003**, 3099.
[77] R. A. Swanson, R. S. Haywood, J. B. Gibbons, K. E. Cordova, B. O. Patrick, C. Moore, A. L. Rheingold, C. J. A. Daley, *Inorg. Chim. Acta* **2011**, *368*, 74.
[78] M. R. J. Elsegood, A. J. Lake, M. B. Smith, *Dalton Trans.* **2009**, 30.
[79] L. Bemi, H. C. Clark, J. A. Davies, C. A. Fyfe, R. E. Wasylishen, *J. Am. Chem. Soc.* **1982**, *104*, 438.
[80] J. R. L. Priqueler, I. S. Butler, F. D. Rochon, *Appl. Spectrosc. Rev.* **2006**, *41*, 185.
[81] N. D. Knöfel, H. Rothfuss, J. Willenbacher, C. Barner-Kowollik, P. W. Roesky, *Angew. Chem. Int. Ed.* **2017**, *56*, 4950; *Angew. Chem.* **2017**, *129*, 5032.
[82] L. G. Scanlon, Y. Y. Tsao, K. Toman, S. C. Cummings, D. W. Meek, *Inorg. Chem.* **1982**, *21*, 2707.
[83] V. T. Annibale, D. A. Dalessandro, D. Song, *J. Am. Chem. Soc.* **2013**, *135*, 16175.
[84] V. T. Annibale, D. Song, *Organometallics* **2014**, *33*, 2776.
[85] M. Iglesias, C. Del Pino, S. Garciá-Blanco, S. Martínez Carrera, *J. Organomet. Chem.* **1986**, *317*, 363.
[86] H. Jiang, E. Stepowska, D. Song, *Eur. J. Inorg. Chem.* **2009**, 2083.
[87] S. O. Grim, R. A. Ference, *Inorg. Chim. Acta* **1970**, *4*, 277.
[88] M. B. Ezhova, B. O. Patrick, B. R. James, *Organometallics* **2005**, *24*, 3753.
[89] C. Fischer, C. Kohrt, H.-J. Drexler, W. Baumann, D. Heller, *Dalton Trans.* **2011**, *40*, 4162.
[90] C. Kohrt, S. Hansen, H.-J. Drexler, U. Rosenthal, A. Schulz, D. Heller, *Inorg. Chem.* **2012**, *51*, 7377.
[91] J. C. Koziar, D. O. Cowan, *Acc. Chem. Res.* **1978**, *11*, 334.
[92] R. Usón, A. Laguna, A. Navarro, R. V. Parish, L. S. Moore, *Inorg. Chim. Acta* **1986**, *112*, 205.
[93] R. Melanson, F. D. Rochon, *Can. J. Chem.* **1975**, *53*, 2371.
[94] C. Zovko, Master's thesis, Karlsruher Institut für Technologie (KIT), **2018**.
[95] A. Görner, Bachelor thesis, Karlsruher Institut für Technologie (KIT), **2017**.
[96] P. S. Pregosin, R. W. Kunz, *^{31}P and ^{13}C NMR of Transition Metal Phosphine Complexes*, Springer, Berlin, **1979**.
[97] R. H. Crabtree, *The Organometallic Chemistry of the Transition Metals*, 5th ed., Wiley, New Jersey, **2009**.

Manuscript received: March 18, 2020
Accepted manuscript online: April 14, 2020
Version of record online: August 31, 2020

© 2020 The Authors. Published by Wiley-VCH GmbH